

PHASE SEPARATION IN AQUEOUS-ORGANIC
NANODROPLETS

BY

YAKUBU SANI WUDIL

A Thesis Presented to the
DEANSHIP OF GRADUATE STUDIES

KING FAHD UNIVERSITY OF PETROLEUM & MINERALS

DHAHRAN, SAUDI ARABIA

In Partial Fulfillment of the
Requirements for the Degree of

MASTER OF SCIENCE

In
PHYSICS

NOVEMBER 2016

KING FAHD UNIVERSITY OF PETROLEUM & MINERALS

DHAHRAN 31261, SAUDI ARABIA

DEANSHIP OF GRADUATE STUDIES

This thesis, written by YAKUBU SANI WUDIL under the direction of his thesis advisor and approved by his thesis committee, has been presented to and accepted by the Dean of Graduate Studies, in partial fulfillment of the requirements for the degree of MASTER OF SCIENCE IN PHYSICS.

Thesis Committee



Dr. Abdullah A. Al-Sunaidi

(Department Chairman)

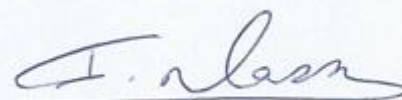


Dr. Fawaz Hrahsheh (Advisor)



Prof. Salam A. Zummo

(Dean of Graduate studies)



Prof. Dr. Ibraheem M.A. Nasser (member)



Dr. Abdallah M. Al-Zahrani (member)

Date

30/11/16

© Yakubu Sani Wudil

2016

Dedicated to

My beloved and ever loving parents for their love, support, encouragement and sound moral training,

My teachers at all levels for preparing me to attain this success,

My Brothers and sisters for their support and encouragement at all times,

My colleagues at all levels, friends and well-wishers for their positive contributions in one way or the other.

ACKNOWLEDGEMENTS

In the name of Allah, the beneficent, the most merciful, all praise is due to Allah in Him we seek guidance and refuge from all evil. May His blessings be upon his noble prophet Muhammad (S.A.W), his family, companions and all those that follow his path up to the day of resurrection. I thank Him for sparing my life in full comforts to carry out this thesis work.

My most sincere gratitude goes to my indefatigable thesis advisor Dr. Fawaz Hrahsheh who has selflessly and painstakingly contributed positively toward the accomplishment of this work, and above all for his understanding, patience, guidance and encouragement throughout the programme.

I must thank my late father Alhaji Sani Muhammad Wudil and My mother Hajiya Hauwa Ibrahim for all they have done for me to witness this day. May Allah grant them Jannatul Firdous. Without their help this piece of work will not have seen the light of the day.

To my thesis committee members, Prof. Dr. Ibraheem Nasser and Dr. Abdallah Al-Zahrani, I am profoundly grateful for your positive comments and your friendly atmosphere. I must also acknowledge the contributions of all my Lecturers whose efforts and contributions are highly fruitful, history will never let your efforts go with no spirit of remembrance.

I must also appreciate the efforts of all family members, friends at home and in school as well, and well-wishers who helped in one way or the other to make this success a reality.

I am also thankful to my employers, Federal university, Dutse, Nigeria for the fellowship opportunity.

Finally, I am fully indebted to the management of King Fahd University of petroleum and Minerals and the ministry for higher education, Saudi Arabia for the Scholarship opportunity given to me and all the necessary support to accomplish my master's degree.

TABLE OF CONTENTS

ACKNOWLEDGMENTS.....	iv
TABLE OF CONTENTS.....	vi
LIST OF FIGURES.....	viii
LIST OF TABLES	ix
THESIS ABSTRACT.....	x
ملخص الرسالة.....	xi
CHAPTER 1 INTRODUCTION.....	1
1.1 Background and Applications.....	1
1.2 Binary Nanodroplet Structures.....	7
1.2.1 Large Nanodroplets.....	8
1.2.2 Small Critical Nuclei.....	10
1.3 Thesis Objectives.....	13
1.4 Thesis Motivations.....	13
CHAPTER 2 THEORY OF MOLECULAR DYNAMICS SIMULATIONS.....	15
2.1 Molecular Dynamics Equations of Motion.....	16
2.2 Lennard-Jone’s Potential	18
2.3 Surface Tension.....	21
CHAPTER 3 MOLECULAR DYNAMICS SIMULATIONS.....	23
3.1 Methodology.....	23
3.2 MD of Pure Butanol.....	23

3.3 MD of Water-Butanol Planar Interfaces.....	25
3.4 MD of Water-Butanol Nanodroplets	28
CHAPTER 4 CONCLUSIONS AND RECOMMENDATIONS.....	33
4.1 Conclusions.....	33
4.2 Recommendations.....	34
References.....	36
Vitae.....	41

LIST OF FIGURES

Fig. 1: Dimensionless density profiles of (a) A well-mixed structure. (b) A core-shell structure...	3
Fig. 2: A structural phase diagram for aerosol nanodroplets.....	3
Fig. 3: A cross-section view of the tube shows separation elements [http://twisterbv.com/].....	7
Fig. 4: Snapshot of MD simulation of a nanodroplet containing 1000 water molecules and 500 nonane molecules at $T = 260 \text{ K}$	10
Fig. 5: Schematic diagram of the Lennard-Jones's potential.....	19
Fig. 6: Temperature dependence of butanol surface tension γ	24
Fig. 7: Temperature dependence of butanol equilibrium density ρ	25
Fig. 8: Snapshot of the initial configuration of the water-butanol mixture at $t=0.0\text{ns}$	26
Fig. 9: Snapshot of the final configuration of the water-butanol mixture after 100ns	26
Fig. 10: Density profile of the water-butanol bulk structure at $T=295\text{K}$	27
Fig. 11: Snapshot of the Core-shell Structure of the spherical nanodroplets for 200 Butanol and 100 Water molecules at $T=250\text{K}$	29
Fig. 12: Snapshot of the Phase-separation Structure of the spherical nanodroplets for 1000 Butanol and 1000 Water molecules at $T=250\text{K}$	30
Fig. 13: Number density map around a symmetry axis connecting the center of water-rich phase and the butanol-rich phase.....	30
Fig. 14: Snapshot of the Well-Mixed Structure of the spherical nanodroplet for 3000 Butanol and 1000 water molecules at $T=250\text{K}$	31
Fig. 15: Snapshot of the Well-Mixed Structure of the spherical nanodroplets for 1000 Butanol and 1000 water molecules at $T=295\text{K}$	32

LIST OF TABLES

Table 1: Lennard Jones Parameters of TraPPE butanol with ϵ' as the water oxygen-butanol cross interaction LJ parameters.....	27
--	----

THESIS ABSTRACT

NAME: Yakubu Sani Wudil

TITLE OF STUDY: Phase separation in aqueous-organic nanodroplets

MAJOR FIELD: Physics

DATE OF DEGREE: JANUARY, 2017

Supercooled and nano-confined water occur frequently as nanometer-sized aqueous-organic aerosol droplets that are ubiquitous in the atmosphere and in many industrial processes such as natural gas refining. Nanodroplet structure is important because it influences droplet growth, evaporation rates, nucleation rates, and radiative properties. We used classical molecular dynamic simulations to study the structure of binary water-butanol nanodroplets for several temperatures and droplet sizes. Water-butanol interactions are modeled using a LJ potential with energy and size parameters adjusted to reproduce experimentally observed mutual binary solubility of equilibrium water-butanol system at room temperature. To compare with the results of the density functional theory (DFT) [*Phys. Chem. Chem. Phys.*, **8**, 1266-1270 (2006)], we focus on $T=250$ K. Our simulations show three different structures according to the butanol concentrations. For low concentrations, we observe a core-shell (CS) structure where a butanol shell completely wets a rich water core. For high concentrations, perfect well-mixed (WM) structure occurs as the water and the butanol become highly miscible. For intermediate concentrations of butanol, we found a distinct phase separated (Russian Doll)-Shell (RDS) structure for water/butanol nanodroplets. This RDS structure consists of a nearly spherical rich water droplet partially wetted by a well-mixed water/butanol convex lens (RD) and this lens-on-sphere structure is coated by a thin shell of butanol. Moreover, we study the stability of our RDS structure for higher temperatures.

الرسالة ملخص

تحدث عملية التبريد الفائق والحبس النانوي للماء على شكل قطرات مائي-عضوية نانوية الحجم حيث تنتشر في كل مكان داخل الغلاف الجوي وفي مجالات صناعية عديدة. أهمية معرفة البنية التكوينية للقطرات النانوية يعزى الى انها تأثر على عدة ظواهر طبيعية مثل معدل نمو القطرات ومعدل التبخر ومعدل تكون النوى التي تشكل اجنة لتحول المادة من حالة الى أخرى بالإضافة الى الخصائص الاشعاعية للقطرات. لقد استخدمنا طريقة محاكاة الديناميكا الجزيئية المحوسبة لدراسة بنية هذه القطرات لعدة درجات حرارية وتراكيز مختلفة للبيوتانول العضوي. لقد قمنا بمعايرة المعاملات اللازمة في اقتران لينارد-جونز لحساب التفاعل بين الماء والبيوتونال حيث قمنا باعتماد المعاملات التي أعطت مستوا امتزاج مناسب بين المركبين عند حرارة الغرفة. ولكي نقارن نتائجنا مع نتائج نظرية الكثافة الوظيفية (DFT) (*Phys. Chem. Chem.*) [Phys. Chem. Chem. (2006) 8, 1266-1270] قمنا بالتركيز على درجة الحرارة ٢٥٠ درجة مطلقة. عند درجات حرارية منخفضة، تم رصد ثلاثة اشكال بنيوية مختلفة للقطرات النانوية حسب تركيز البيوتانول. فعندما يكون تركيزه قليلا، فإنه يكون قشره تغطي نواة غنية بالماء. بينما يختلط البيوتانول والماء تماما عند التراكيز العالية. اما الشكل البنيوي المميز فيحدث عند التراكيز المتوسطة حيث يحيط مزيج من الخليط بنواة غنية بالماء ويغلفها قشرة رقيقة من البيوتونال.

CHAPTER ONE

INTRODUCTION

1.1 Background and Applications

A number of molecular computational works for the study of liquid/vapor interfaces have been presented in many literatures. However, not many are reported for liquid/liquid interfaces. Molecular Dynamics (MD) simulation of Hexane/water interface has been reported in the work of Carpenter and Hehre [1]. They noticed that few molecules of hexane was surrounded by water, which is not in agreement with the conventional characteristics of the solubility of hexane in water and attributed the inconsistency to the type of intermolecular potentials employed i.e. standard Optimized Potentials for Liquid Simulations (OPLS) and Simple Point Charge (SPC) parameters. Meyer and his team [2] investigated two immiscible liquids through employing two identical Lennard-Jone's (LJ) potentials. They used modified LJ potential in order to vary the liquids' miscibility to compute the interactions between two atom types (L1 and L2). They concluded that reduced miscibility is resulted through reducing the attractive part of the potential.

The spatial arrangement of different kinds of species in a droplet plays a vital role on the interaction of the particle with its environment. Contemporary researchers in the field of aqueous-organic nanodroplets have focused mainly on organic species that are *partly soluble* in water. The mixtures exist in two phases having miscibility gaps; the water rich layer (L1) and the organic rich layer (L2) whose composition is dependent on the type of the organic substance. As revealed in the experiment of Small Angle Neutron Scattering (SANS) [3] and in theoretical

Density Functional Theory (DFT) [4] studies and Lattice Monte Carlo simulations [5] made for a model of binary structures that follow these characteristics, such non ideality is capable of creating internal structures in nanodroplets.

The DFT section considers the model as a system consisting hard spheres with Yukawa attractive forces. The choice of the force parameters and the sphere diameters was made such that the result agrees with measured surface tensions, vapor pressures and densities of pure bulk water and pentanol at 250 K [4]. The properties of the binary nanodroplets was then determined through the application of mean field DFT. Analysis of the results shows that the model of the water-pentanol matches the traits of the real water-pentanol mixture.

Two main classes of droplets were discovered [4], the well mixed (WM) and Core-shell (CS) structures as shown in Fig. 1 for two average sized nanodroplets. For the well-mixed structure, the density profiles are somewhat flat throughout the droplet. Towards the vapor liquid interface, the water density decays rapidly leaving behind a mostly pentanol coating on the droplet surface. These structures mimic the bulk L2-vapor interface. In the same vein, the (CS) structure mimic the bulk L1-Vapor interface and agrees with the SANS measurements [3] in that the core contains plenty water and the concentration of the pentanol remains less until the vapor-liquid interface is attained. At the interfacial zone, the density of the water falls significantly while pentanol density profile is approximately a Gaussian shaped adsorbed layer. The thickness and density of this adsorbed layer change with the pentanol vapor concentration.

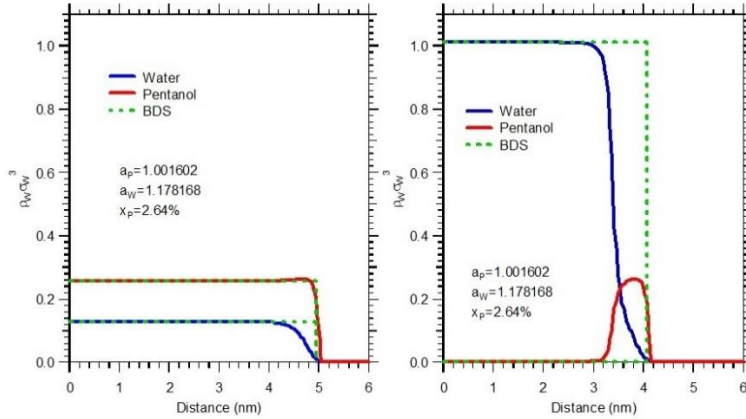


Fig. 1: Dimensionless density profiles of (a) A well-mixed structure. (b) A core-shell structure [4].

The above figure shows the density profiles of critical droplets at vapor state activities $a_p= 1.002$, $a_w= 1.178$ where $a_i=P_i/P_{i0}$ with P_i and P_{i0} actual and equilibrium vapor pressures of species i , respectively. The mol% of pentanol is 2.64% in the bulk gas phase. The dashed line describes the droplet size. The structures exist at the same temperature and vapor composition.

From the DFT study of the water-pentanol mixture, a bi-structural region of both the well-mixed and core-shell is determined where the pentanol concentration is moderate [4]. In this region, *any* of these classes of structures is bound to exist. The structural phase diagram for aerosol nanodroplets is shown in Fig. 2. The thick lines represent the vapor Binodal compositions.

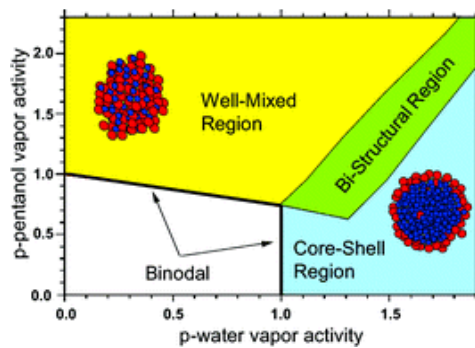


Fig.2: A structural phase diagram for aerosol nanodroplets [4].

In the bi-structural zone, either of the droplets can exist at the same vapor state but with different free energies. For the top left and bottom right, only the well-mixed and core-shell structures can be found, respectively. For the purpose of this work of water-butanol, the bi-structural region can be explored by varying the concentration of butanol at constant water concentration and temperature using canonical (NVT) molecular dynamics simulations.

One of the major energy sources in Saudi Arabia is the natural gas. In addition to methane, which forms the primary constituent of the natural gas mixture, the gas contains many other compounds like butanol, ethane, propane, water and higher aqueous-organic clusters. Each component of the mixture is of particular significance for various industrial and domestic usages. The conventional options for separation of this mixture involves use of chemicals or lowering the dew point of the natural gas (the temperature at a given pressure) at which the hydrocarbon components of any hydrocarbon-rich gas mixture start to condense out of the gaseous phase by removing water and hydrocarbon condensates. In both cases, the processing equipment is large and requires skilled work force.

The emergence of supersonic separation in the gas industry has become outstanding owing to its effectiveness and environmental safety. For a given pressure, each constituent has its condensation temperature. Hence, the principle of separation of this mixture into various components requires cooling the flow to the desired temperature [6]. The supersonic separation involves cooling the gas to induce droplet formation and growth in the separation chamber, a cyclonic gas/liquid separator to capture the condensate and a diffuser to recompress the dried gas and keep the overall pressure loss across the device to ~25%. This mechanism has several advantages over the conventional ones in that, they do not require use of chemicals, they have no moving parts and they are not heavy compared to the traditional mechanism [7].

As the separation goes supersonic, key questions remain pertaining droplet formation and growth rates in the vapor mixture, these questions are not unconnected with the droplet structure. The literature shows that hydrocarbons can inhibit water condensation because they wet the water surface to a good extent but the water only poorly wets the hydrocarbon surface [8], [9]. On the other hand, high pressure methane reduces the interfacial tension between organic and aqueous phases, thereby modifying the droplet structure and hence affecting the nucleation and growth. Recent studies of species with small miscibility reveals that three types of structures can form; well mixed, core-shell and a non-spherical, partially segregated structure termed “Russian doll” (RD) structure depending on the vapor composition, temperature, miscibility and the interfacial tensions of the species [4], [10].

The primary concern of this work is therefore to investigate, using molecular dynamic simulation, the structures of organic nanodroplets, particularly water-butanol nanodroplets, created in this separation method in highly non-ideal water-butanol systems under conditions equivalent to those found in the supersonic separators with a view to improving the energy efficiency of natural gas production.

The field of droplets is increasingly drawing attention of researchers particularly in the specialty of aerosol science, atmospheric science and natural gas production. This is due largely to the existence of several components in the mixture. Several compounds interact uniquely with other constituents of the complex mixture based on their miscibility and other distinguishing properties such as vapor pressure and structure.

Recently, natural gas separators have been developed [6] that combine (1) a supersonic expansion of a swirling flow to cool the gas and induce droplet formation and growth, (2) a cyclonic gas/liquid separator to capture the condensate, and (3) a diffuser to recompress the dried gas and keep the overall pressure loss across the device to ~25%. Worldwide, five of these devices are now in commercial operation. The oldest, operating in East Malaysia since 2003, processes 600 MMSCFD of sour gas on an offshore platform [6]. **Twister BV** (<http://www.twisterbv.com/>), is the world leader in developing and implementing this technology.

The tube, Fig. 3, is the heart of the system that combines adiabatic cooling, in which no heat enters or leaves the system, with cyclonic separation in a single, compact device. Adiabatic cooling is accomplished through a Laval nozzle — an aerodynamically shaped venturi tube which achieves an isentropic expansion efficiency of more than 80%. The swirling motion is generated by a fixed static vane ring at the entrance of the Laval nozzle. The swirl strength increases strongly due to the contraction in the nozzle, resulting in a centrifugal field of around 500,000g. The fine dispersed liquids formed during the adiabatic expansion and cooling are separated as a result of the centrifugal forces exerted by the strong swirling flow, and removed from the dry flow at minimum temperature and pressure with significantly high separation efficiency. At the point where liquid/gas separation takes place, the total fluid velocity is around 1,312 ft/second (400 m/second) resulting in a maximum gas residence time inside the tube of less than 2 milliseconds. The remaining kinetic energy in the separated flows within the tube is transformed to increased static pressure in the diffuser sections.

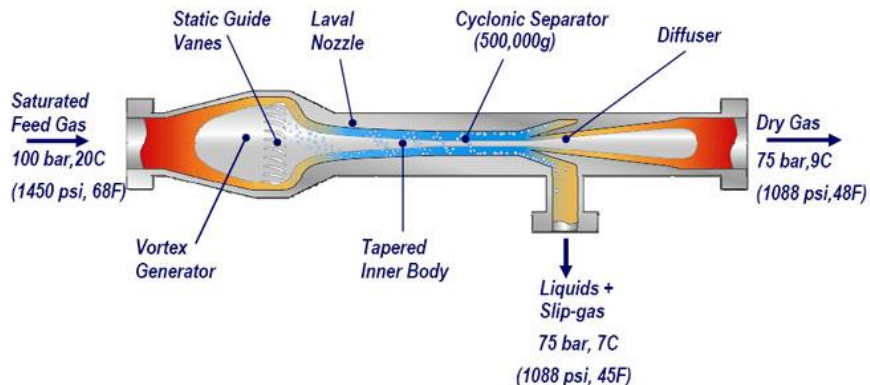


Fig. 3: A cross-section view of the tube shows separation elements [http://twisterbv.com/].

1.2 Binary Nanodroplet Structures

The structural studies of nanodroplets generally provides broader picture to the spatial distributions of the various chemical species inside the droplet. The concept is mostly applied for droplets having many thousands down to tens of molecules. The energy of formation of the droplets is strongly influenced by the structure. This in turn has a major effect on the rates of droplets growth, evaporation as well as the nucleation rate. The interactions of aerosol droplets and their environments are also affected by the structure. This influences phenomena such as trace gas adsorption and uptake, heterogeneous chemistry and radiative characteristics of bigger droplets. In this work, we focus on understanding the structures in highly non-ideal water-butanol systems using molecular dynamics simulations.

There is increasing and considerable evidences for the existence of multicomponent homogeneous nucleation of particles [11]–[13]. Under the normal circumstances, these particles would eventually increase in size to several nanometer size ranges up to the time they turn to Aitken nuclei. Continuous size increase of these particles may lead to the formation of cloud condensation nuclei. Despite the broad research in the field, some of the details are however still

unclear, and will depend on the atmospheric chemical compositions and local thermodynamics conditions to mention but few. It is evident that partial pressures, temperature and chemical identity of the species present play a great role on growth rates and particle nucleation. These factors also firmly affects the critical nuclei's structure and of the larger post critical droplet.

1.2.1 Large Nanodroplets

Recent theoretical and experimental studies conducted with a view to exploring aqueous-organic nanodroplets structure are strongly facilitated by the atmospheric significance of these systems [14], [15]. Ideally, the organic systems are not considerably soluble in water. They are only sparingly soluble for non-bulk mixtures. For the bulk specie mixtures, there exists a miscibility gaps between organic-rich and water-rich phases. The composition of the organic-rich layer depends on the organic species' nature. The phase behavior makes one to expect the existence of non-uniform distribution of the organic particles in the water-rich phase of the aqueous-organic aerosol droplet. It can exist in the form of aqueous core inside organic material shell [16]. The existence of such core-shell structures has been supported experimentally from SANS measurements on moderately miscible species of water/n-butanol [17] and even more evidence from surface analysis of atmospheric aerosol particles [18]. The structures of aqueous organic nanodroplets that can exist under various conditions have been immensely explored by two recent theoretical studies. Both lattice Monte Carlo and DFT techniques were employed to deal with binary fluid models that imitated the properties of slightly miscible aqueous-organic systems [19].

The DFT of Wilemski and Li [4] is based on attractive Yukawa forces existing between the binary mixtures of hard spheres. This means is a continuation on the work of spherical droplet of

Sullivan's theory [20] of interface for binary Vander-Waal's fluid. It is closely related to the DFT of Oxtoby and Zeng [21] for nucleation in binary fluid. and it generalizes the work of Oxtoby et al. [22] for unary systems. In these theories, the species density defines the grand potential. The type of the dependence defines the complexity of the evolving Euler-Lagrange equations that have to be solved in order to get the droplet density profiles at equilibrium. The simplest and earliest functionals require the local density and random phase approximations.

The effect of temperature on the structure of nanodroplets has recently been addressed in the work of Ning and Wilemski [4]. They carried out Monte Carlo simulations of model aqueous nanodroplets having approximately 4000 particles. Their work is a generalization of the previous lattice Monte Carlo work of Pakula and Cordeiro [23] who conducted their simulation on unary droplets. They used a simple FCC model having nearest neighbor interactions.

Recent MD simulations and cylindrical coordinates DFT have demonstrated that nanodroplets containing immiscible water and nonane are non-spherical and highly phase separated [24]. The 'Russian doll', Fig.4, structure may be simply modeled as a spherical nonane lens that partially wets a spherical water droplet. Nonetheless, the partial miscibility of water-butanol has greatly lead to different structures (WM and CS). Consistent with the spherical coordinates DFT [4], the structure of our water-butanol nanodroplets are expected to be well mixed and core-shell for large and small butanol concentrations, respectively. However, for relatively reasonable intermediate concentrations, a new structure *different* from the Russian-doll is expected resulting from the partial miscibility of the water-butanol mixture and also does not belong to the bi-structural scenario [10].

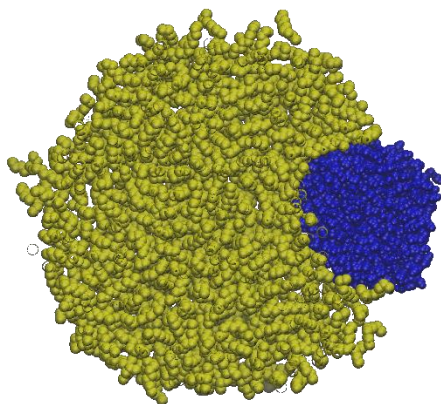


Fig. 4: Snapshot of MD simulation of a nanodroplet containing 1000 water molecules and 500 nonane molecules at $T = 260$ K [10].

1.2.2 Small Critical Nuclei

The binary critical nuclei usually consists 30-100 molecules for typical ideal experimental conditions. The impact of structure in these cases can be easily appreciated by noting the famous effect of surface enrichment in water-alcohol system. The molecules of alcohol concentrate at the interfaces of vapor-liquid of bulk droplets and small systems decreasing their interfacial tension. This strongly reduces the job of critical nucleus formation in binary nucleation, hence leading to the famous mutual enhancement of nucleation [25]–[28]. However, after using phenomenological models for the surface composition, significant progress has been made [29]–[33]. The structure in terms of compositional variables has been successfully explained by Laaksonen and Kulmala model [5]. This type of models reveals only a simple characterization of the cluster structures. However, for detail spatial resolution, treatment at microscopic levels needs to be involved based on molecular dynamics simulation or statistical mechanics.

The comprehensive demonstration of surface enrichment can best be attained using computational methods such as Monte Carlo (MC) or molecular dynamics (MD) techniques [34], [35], which generate computer-processed images of the clusters. Apart from visualization facility, these methods enable them to study quantitatively, for quite realistic model systems, the complete effect of cluster structure on the process of nucleation. For systems governed by complex and realistic intermolecular potentials, recent developments in Monte Carlo sampling process developed by Chen et al. [36] and by McKenzie and Chen [37] permit the construction of the free energy surface on which nucleation occurs. This possibility allows comprehensive investigations of nucleation mechanisms and pathways under conditions similar to those investigated experimentally. More recently, study of water/ethanol nucleation reproduced the mutual enhancement effect having results that bear reasonable quantitative and excellent qualitative agreement with the experimental activities [36], [37].

In the water/alcohol systems, surface enrichment is a lucid indication of non-ideal thermodynamic property [38]. There are even more fascinating structural effects at extreme non ideality i.e. in nearly immiscible and partially immiscible systems. Ray and his team [39] used classical nucleation theory and discovered that the free energy surface of a partially miscible system could have double saddle points, impliedly, there could be two types of mixed critical nuclei for the particular vapor state. Even though classical nucleation theory is extremely powerful in understanding how the double saddle points relates to the kinetics of nucleation, it however could not uncover the structures of the critical nuclei. Clarke and his team [34] discovered multitude different structures at low temperature in a remarkable Monte Carlo/molecular dynamics study on small Lennard-Jones binary clusters that might evolve depending on the energy strength of the Lennard-Jones potential. Some of the types discovered

were surface-enriched droplets, well-mixed droplets and phase-separated, non-spherical droplets. Despite the worth of these insights into the cluster structure's energetics, they are somewhat worthless with regards to the nucleation process because there is no evidence that these cluster structures may exist as critical nuclei. Talanquer and Oxtoby have provided insight in this direction [22]. They studied binary nucleation of partially miscible Lennard-Jones systems using density functional theory in the square gradient approximation. They also studied the behavior of double saddle points. In addition, they found phase-separated, non-spherical droplets in agreement to those of Clarke and his Colleagues [34]. In the Monte Carlo simulations by Frenkel and Wolde and more advanced density functional theory findings by Laaksonen and Napari for binary Lennard Jones clusters indicated that the phase separated cluster structures were not critical nuclei rather corresponded to local maxima on the free energy surface, therefore not significant for nucleation [40], [41]. It is worth noting that all the works carried out by Napari and Laaksonen [42], Talanquer and Oxtoby [43] and by Frenken and Wolden [40] were executed at single, moderately high temperature nearly twice as that used in the research of Clarke and his colleagues [34]. Therefore, even though phase separated, non-spherical Lennard Jones droplets may not exist as critical nuclei at temperature close to the triple point, the eventuality however still needs to be addressed at low temperatures.

In the recent study conducted by Chen and McKenzie [37], they addressed some of these prevailing issues. They studied alcohol-nonane system, and they observed strange behavior at 230K temperature, which coincides with the low temperature utilized in the work of Viisanen and his team [44]. The saddle region on the free energy surface was observed to be flat and broad for small range of vapour condition, leaving unclear the conception of a single critical nucleus having well defined composition. The case continued at 300K and reduced to some extent at

360K. They identified at 230K, a subset of clusters with equal number of ethanol and n-nonane molecules. They also observed similarity of the cluster structures with nonspherical, phase-separated Lennard Jones droplets discovered by Clarke et al [34] and Talanquer and Oxtoby [22]. These compositions rest on the saddle's flat part. However, they did not reveal high temperature critical nuclei structure.

1.3 Thesis Objectives

The major goal of this thesis project is to investigate on the properties of droplets particularly Aqueous-organic nanodroplets created in the contemporary process of natural gas separation methods by studying their formation and structure in highly non-ideal water-butanol systems under conditions equivalent to those found in the supersonic separators. The work would also present reliable information on nanodroplets activity to the field of cloud and atmospheric physics. The work focuses on the changes of the water-butanol nanodroplets structures by altering the butanol concentration and varying the temperature values applying NVT molecular dynamics simulations.

1.4 Thesis Motivations

Saudi Arabia is one of the leading nations in the production of natural gas which is majorly consumed within the country for domestic and industrial purposes. This gas is made of mixtures of Methane, water and higher hydrocarbons. Hence, the need for refining this gas to extract the desired dry gas arises. Conventionally, the separation methods involve either the use of chemicals or reducing its dew point. The processes involve use of very large equipment besides the consequence of the use of chemicals to the environment. An alternative to the aforementioned techniques is the modern supersonic expansion separation technique. It involves

cooling the gas in a supersonic expansion chamber to trigger droplet formation and growth, isolate the droplets from the gas and re-compress the gas using diffuser to limit pressure losses. The supersonic separator does not require use of chemicals, have no moving parts and is smaller than the traditional processes [6], [7], [45]. As this method gets into operation, a number of unanswered questions rise pertaining the formation and growth of droplets in the complex mixture of the gas, this question would be best answered by studying the droplets structure. In addition to the impact of the work on improving natural gas production efficiency, the project would be of interest to researchers in the field of atmospheric physics, cloud, aerosol science and nucleation.

CHAPTER TWO

THEORY OF MOLECULAR DYNAMICS SIMULATIONS

The concept of Molecular dynamics (MD) simulation was initiated by Fermi, Pasta and Ulam in 1950s and Rahman in 1960 [46], [47]. They used IBM 704 computer to investigate the elastic collisions existing between hard spheres. Gibson and his team used cohesive force surface along with Born-Mayer type of repulsive interaction to simulate radiation damage of solid copper [48]. In the 1964, a landmark simulation of liquid argon was published by Rahman [49], where he used Lennard-Jones (LJ) potential and calculated the properties of the system such as coefficient of self-diffusion and his result was in good agreement with experiments.

The MD simulation is a computer based technique adopted for the studies of the physical motion of atoms and molecules, it is therefore a many body simulation process. The method entails study of the dynamics of the atoms from their interaction for a given interval of time. For a system of interacting particles, the method involves solving numerically, the Newton's equation of motion and the Lagrangian for the system in order to obtain the trajectories of the atoms and molecules. The potential energies of the particles and the forces between the ensembles are obtained from the interatomic potentials [47].

Molecular systems generally involve large number of particles. Therefore, it is not feasible to make analytical approach in order to study the properties of such a system. The introduction of the MD simulation could circumvent such difficulty by using numerical approach. Nevertheless, long duration MD simulations sometimes come with a mathematical complications caused by numerical integration generating cumulative errors. However, this can be reduced by proper

selection of parameters and using appropriate algorithm. For the molecules that exhibit ergodicity, the result of a single MD simulation can be used to find the macroscopic thermodynamic variables of the system [50].

The application of molecular dynamics simulation cannot be overemphasized. It started from the field of theoretical physics and got to be promising in the field of biophysics, material science and biochemistry [51]. The technique is being utilized in the refining of three-dimensional protein structures and other macro molecules using the experimental conditions from Nuclear Magnetic Resonance (NMR) spectroscopy or X-ray crystallography. However, in physics, the widest application of MD simulation is in the studies of the dynamics of phenomena which are mainly at atomic scale, such as ion sub plantation and thin film growth. Such phenomena cannot be examined directly due to their microscopic nature. The Physical properties of materials at nanoscale can also be examined. The process is crucial in structural biology and biophysics such that the motions of biological particles such as nucleic acids and proteins can be carried out. The result can be useful for the interpretation of certain biophysical experimental results and for simulating how the particles interact with other molecules. Principally, MD simulations can be utilized for ab initio of protein structures by modeling folding of the polypeptide chains [50], [52]–[54].

2.1 Molecular Dynamics Equations of Motion

The method of molecular dynamics simulation employs step-by-step solving numerically of Newton's classical equation of motion for the interacting particles to describe the investigated system [55]. The particles which in their simplest case could be atoms or molecules follow the equations:

$$m \frac{d^2 \mathbf{r}_i}{dt^2} = F_i(r_1, r_2, \dots, r_N), \quad (1)$$

where F_i is the force acting upon N particles, \mathbf{r}_i is the position vector for the i^{th} particle, and m is its mass. For the computation of the forces acting on the atoms, we derive them from the potential functions, $U(r_1, r_2, \dots, r_N)$ describing the potential for particular geometric arrangement of the system,

$$F_i(r_1, r_2, \dots, r_N) = -\nabla_{r_i} U(r_1, r_2, \dots, r_N). \quad (2)$$

This form of the force depicts that the total energy is conserved,

$$E = E_{kin} + U \quad (3)$$

with E_{kin} representing the instantaneous kinetic energy. When there is no external forces, we can represent the potential in its simplest form as sum of pair wise interactions,

$$U = \sum_{i=1, j>i}^N U(r_{ij}). \quad (4)$$

Here, the condition that $j > i$ has been used in order to prevent double counting of the interaction. r_{ij} is the absolute distance from i^{th} to j^{th} particle.

The forces acting on the particles are made of the total interacting forces with the individual particles in the system,

$$F = \sum_{j \neq i}^N f_{ij}, \quad (5)$$

where the individual forces could be computed as

$$f_{ij} = -\frac{du(r_{ij})}{dr_{ij}}. \quad (6)$$

But, from the Newton's 3rd law of motion,

$$f_{ij} = -f_{ji}. \quad (7)$$

However, the computational effort of solving the Newton's equation of motion is directly proportional to N^2 and is in most cases related to the evaluation of forces. In order to minimize the computational difficulty, we can cut the range to give limiting separation beyond which the potential can be neglected [55].

2.2 Lennard-Jone's Potential

This is one of the most prominent pair potential for Van der waal's system, with attractive and Pauli repulsive terms. It consists of parameters σ , the diameter, and ϵ , the potential depth which defines the strength of the interaction. This potential has been used in the early studies of the liquid argon properties. It is the most commonly used potential and it takes the form [56]:

$$U(r_{ij}) = 4\epsilon \left[\left(\frac{\sigma}{r_{ij}} \right)^{12} - \left(\frac{\sigma}{r_{ij}} \right)^6 \right], \quad (8)$$

where r_{ij} is the distance between the interacting particles.

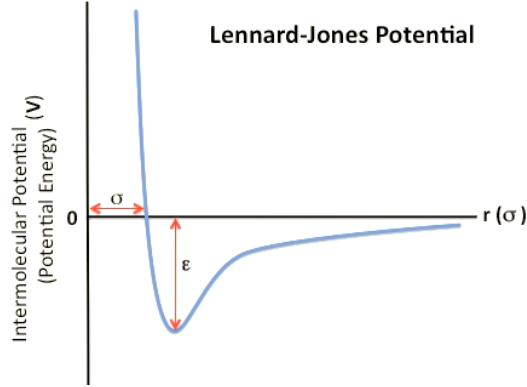


Fig. 5: Schematic diagram of the Lennard-Jones's potential.

As shown in Fig. 5, the potential is predominantly attractive at a relatively long distance, where the 2nd term dominates it. Meanwhile, at shorter distance the potential becomes strongly repulsive with the 1st term, the Pauli repulsive term dominating the potential. The potential cut through zero when r_{ij} equals σ , i.e. $U(\sigma)=0$. However, it reaches its minimum i.e. $U(r_m)= -\epsilon$ at $r_m= 1.1225\sigma$. The choice of the two parameters, ϵ and σ depends on certain physical properties of the system under consideration. For open shell system, the LJ potential is totally inadequate where strong localized bonds are created [49].

The inter particles forces emerging from the LJ potential have the form:

$$f_{ij} = \frac{48}{r_{ij}^2} \epsilon \left[\left(\frac{\sigma}{r_{ij}} \right)^{12} - \left(\frac{1}{2} \right) \left(\frac{\sigma}{r_{ij}} \right)^6 \right] r_{ij}, \quad (9)$$

where the r_{ij}^{-6} term represents the attractive term which dominates the other term at sufficiently large distance. This term mimic the Van der Waal's dispersion forces resulted by dipole-dipole interaction of the fluctuating dipoles. The weak forces give the bonding property of closed-shell systems like krypton and argon [57]. The r_{ij}^{-12} term represents the Pauli repulsive term which

dominates the other term at sufficiently short distance. The term describes the repulsion caused by non-bonded overlap of the electronic orbitals.

In MD simulations, the most widely accepted time integration algorithm is perhaps the so-called Verlet algorithm [56]. The main idea is to present two third-order Taylor expansions for the positions $r(t)$, one backward and the other forward in time. Calling $a(t)$ the accelerations and $v(t)$ the velocities, and b the third derivatives of r with respect to time, one gets:

$$r(t + \Delta t) = r(t) + v(t)\Delta t + \left(\frac{1}{2}\right) a(t)\Delta t^2 + \left(\frac{1}{6}\right) b(t)\Delta t^3 + O(\Delta t^4)$$

$$r(t - \Delta t) = r(t) - v(t)\Delta t + \left(\frac{1}{2}\right) a(t)\Delta t^2 - \left(\frac{1}{6}\right) b(t)\Delta t^3 + O(\Delta t^4).$$

Adding the two expressions gives

$$r(t + \Delta t) = 2r(t) - r(t - \Delta t) + a(t)\Delta t^2 + O(\Delta t^4) \quad (10)$$

And this is basically the so-called Verlet algorithm. Since we are integrating the Newton's equations, the acceleration is just the force divided by the mass, and the force is in turn a function of the position $r(t)$.

$$a(t) = -\left(\frac{1}{m}\right) \nabla V(r(t)) \quad (11)$$

As can be easily seen, the truncation order when evolving the system by Δt is of the order of Δt^4 , even if the third derivatives do not appear explicitly. This algorithm is popular within its type owing to its accuracy, stability and simplicity in implementation.

However, one setback associated with this algorithm is that velocities are not directly generated. Despite the fact that the velocities are not required for the time evolution, their knowledge could sometimes be needed. Moreover, they are needed for the computation of kinetic energy K , whose calculation will in turn be required to test the total energy conservation. This is one of the

essential tests carried out to confirm the accuracy of MD simulation. The velocity can be computed using

$$v(t) = [r(t + \Delta t) - r(t - \Delta t)]/2\Delta t \quad (12)$$

2.3 Surface Tension

Recently, the attention of researchers has been directed toward studying single and binary mixtures of liquid-vapor interface of Van der Waal molecules and atoms interacting via LJ potential. For relatively simple systems having pair-wise additive potentials, the macroscopic characteristics and the quantitative relations between local and molecular interactions have been derived [58].

The interface of binary mixtures of organic compounds can be studied through molecular dynamics simulation. Local pressures profile and surface tension can be found from the process and cast into individual contribution from the molecules. The surface tension would be dependent on the relative strength of the weak Van der Waal's forces. The increasing demand of the studies of thermodynamics and structural properties of liquid-vapor interface is the direct consequence of the fact that there exist some crucial heterogeneous chemical processes occurring at such interfaces. One of the promising applications of the MD simulation is the ability to study carefully the individual interactions of the components for a chosen system and then provide their overall contribution to the interfacial properties [59].

The interfacial region for liquid mixtures is highly disordered and inhomogeneous having only little molecular diameter thickness. This makes it somewhat difficult to determine, quantitatively, the surface composition of the mixture. However, through the use of molecular dynamics

simulation, it is easier to determine the density profiles of the constituents through the interface. Nevertheless, one needs to make comparison between the simulations and the experimental results. Such a link could be given by the surface tension, because it is the quantity which is accessible both experimentally and via simulation [60].

The main expression leading to evaluation of the surface tension is to use the famous relation:

$$\gamma = \left(\frac{1}{n}\right) \int_0^{Lz} \{P_{zz}(z) - [P_{xx}(z) + P_{yy}(z)]/2\} dz \quad (13)$$

Here, n is the number of surfaces, P_{zz} is the normal pressure and P_{xx} (P_{yy}) are the tangential pressure values [61].

CHAPTER THREE

MOLECULAR DYNAMICS SIMULATIONS

3.1 METHODOLOGY

Molecular dynamics simulation technique has been employed to study multicomponent structure. The simulation of the mixture of water-butanol nanodroplets systems was initiated and packed using the Packmol package [62]. The simulation has been carried out with a single-precision compilation of the Gromacs MD simulation package [63]. Using canonical ensemble (NVT) with Periodic boundary conditions, long time simulation of our binary mixture was conducted. The Nose-Hoover algorithm [64] was applied in controlling the system's temperature with a fixed coupling time. The methyl and methylene groups of butanol were treated in the united atom approximation. The Lennard-Jones potential with 1.5 nm cut-off radius was used in governing the short-ranged intermolecular interactions. Similarly, the long-range coulomb interaction has been taken up to the cut-off radius 1.5 nm. The short and long range interactions were managed with twin range cutoff and Particle Mesh Ewald (PME) algorithm, respectively.

3.2 MD OF PURE BUTANOL

Pure butanol ensembles have been studied separately prior to the water-butanol mixture in order to confirm its purity and observe its properties as compared to the standard ones in the literature and experiments [65]. A 500 butanol molecules were considered and the job was submitted for 100 ns at various temperatures ranging from 240-300K. We calculated the surface tension at

each temperature within time average of 80-100ns. The volume of the simulation box used to accommodate the ensembles was $3.1 \times 3.1 \times 20 \text{ nm}^3$.

The values of the surface tension of Transferable Potential for Phase Equilibrium Field (TraPPE) model of butanol, at various temperatures, are plotted and compared to experimental results as presented in Fig. 6. From our analysis, the surface tensions of the model shows a good agreement with experimental data and behaves consistently, like that of the literature, with increased temperature.

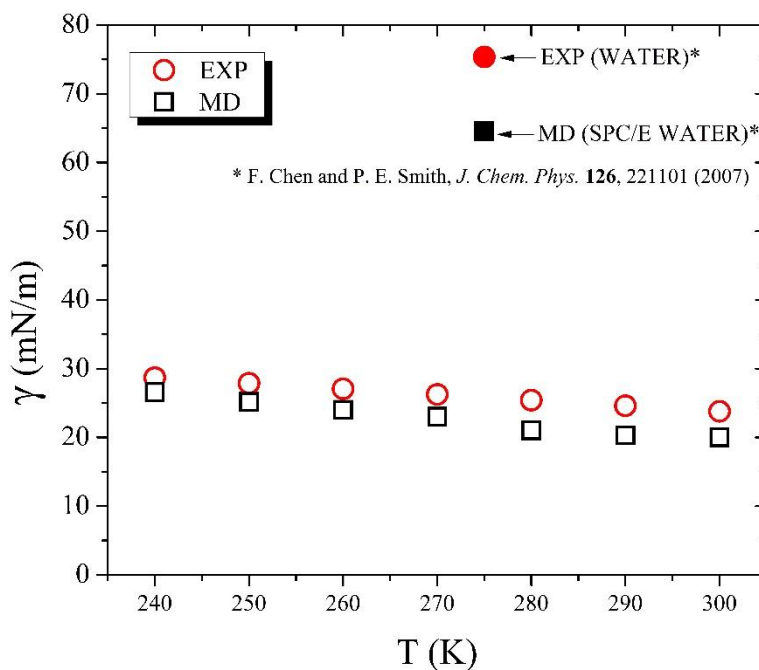


Fig. 6: Temperature dependence of butanol surface tension γ .

Moreover, TraPPE force field is known to give reasonable vapor-liquid coexistence curve [66]. In our simulations, to restudy the liquid part of phase diagram (binodal line), we focus on the butanol equilibrium liquid density variation with temperature (ρ vs. T). As shown in Figure 7, the results are in good agreement with the experimental values specially the behavior with temperature.

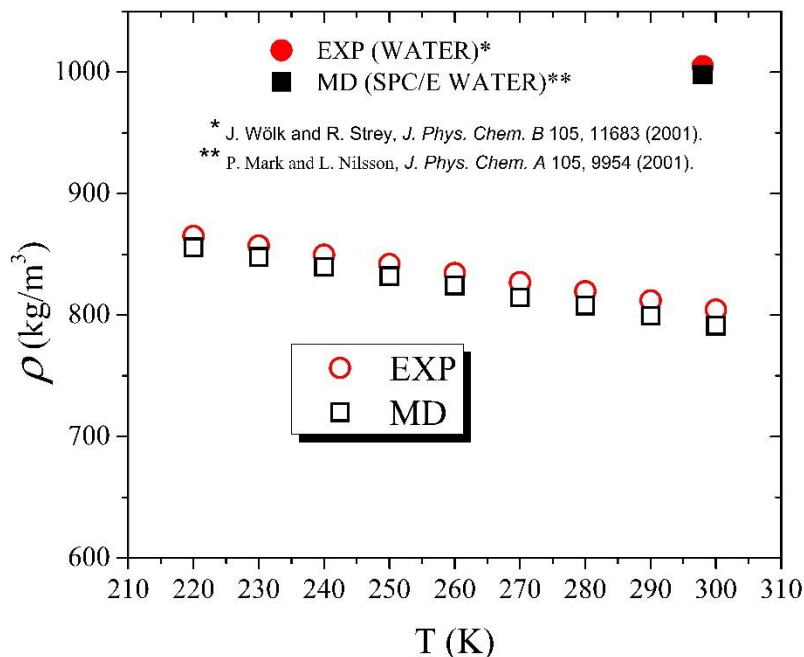


Fig. 7: Temperature dependence of butanol equilibrium density ρ .

3.3 MD OF WATER-BUTANOL PLANAR INTERFACES

The simulation system consists of initial configuration of two slabs of 500 butanol molecules each, sandwiching a slab of 2500 water molecules. The structure was created in form of a box of volume $3.1 \times 3.1 \times 35 \text{ nm}^3$. The Z-axis is situated in such a way that it is perpendicular to the interfaces. For all the three spatial dimensions, Periodic boundary conditions were applied. The snapshot of the initial configuration of WB bulk structure was also presented in Fig. 8, and the final mixture after applying the canonical and molecular dynamics simulations for 100ns is presented in Fig. 9. The former shows the water in between the two butanol phases while the later shows how the two components of the mixture spread into each other according to their respected solubility values.

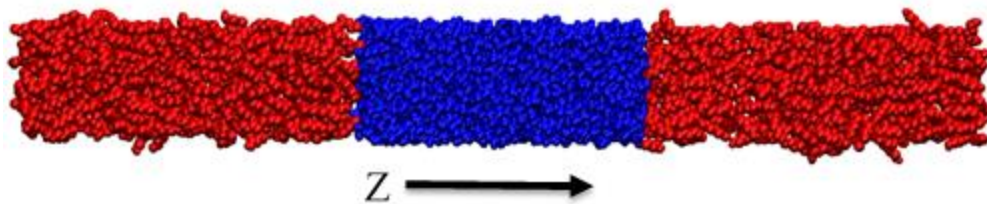


Fig. 8: Snapshot of the initial configuration of the water-butanol mixture at $t=0.0\text{ns}$.

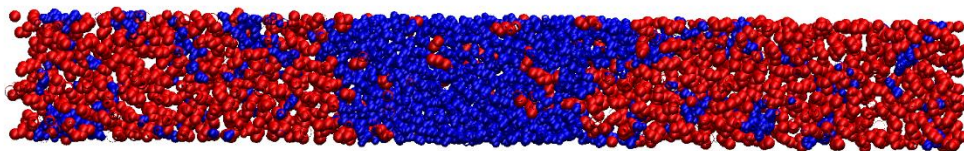


Fig. 9: Snapshot of the final configuration of the water-butanol mixture after 100ns .

Series of molecular dynamics simulations have been carried out on the bulk mixture of butanol and water with a view to study the thermodynamics property and solubility of the two liquids in each other and to identify the sensitivity of the properties to the Lennard Jones's parameters. The solubility of water in butanol, S_{WB} , and the solubility of butanol in water, S_{BW} , can easily be computed from the density profile. Lower repulsion between the oxygen of water and carbon of butanol will generate higher solubility. Understanding these characteristics gives details of the relationship between the macroscopic properties and the van der Waals parameters. Our molecular dynamic simulations were carried for Extended Simple Point Charge (SPC/E) model of water and TraPPE butanol [67]. The water-butanol cross interactions are modeled using LJ potential with energy and size parameters adjusted to reproduce experimentally observed water-butanol mutual solubility at room temperature, Table 1. Here, we only adjusted the cross interaction strengths between water's oxygen atom, ϵ_{OW} , and the neutral (*zero-charge*) butanol's

carbon united atoms as $\epsilon' = \sqrt{\epsilon \epsilon_{OW}} + 0.1$. All other cross interactions strengths were calculated without adjustment as $\epsilon' = \sqrt{\epsilon \epsilon_{OW}}$.

Table 1. Lennard Jones Parameters of TraPPE butanol [68] with ϵ' as the water oxygen - butanol cross interaction LJ parameters.

(pseudo) atom	ϵ [kJ mol ⁻¹]	σ [Å]	q [e]	$\epsilon' = \sqrt{\epsilon \epsilon_{OW}} + 0.1$
[CH3]-CH2-	0.81982	3.750	0.000	0.827867
CH3-[CH2]-CH2	0.38747	3.750	0.000	0.598678
(pseudo) atom	ϵ [kJ mol ⁻¹]	σ [Å]	q [e]	$\epsilon' = \sqrt{\epsilon \epsilon_{OW}}$
CH2-[CH2]-OH	0.38747	3.950	0.265	0.498678
O	0.77824	3.020	-0.700	0.709053
H	0.00000	0.000	0.435	0.000000

With these van der Waal's parameters, we have calculated the density profile for the slabs of the water-butanol mixture over the average timeframe of 80-100ns range of the computation. Fig. 10 shows the plotted density profiles along the Z-side of the simulation box.

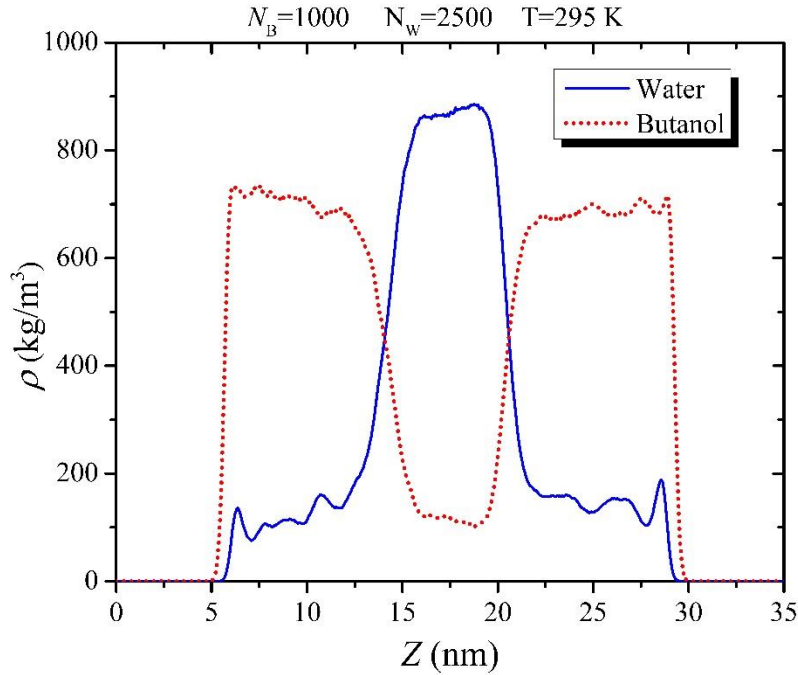


Fig. 10: Density profile of the water-butanol bulk structure at T=295K.

The solubility of water in the butanol was calculated according to the percentage mass fraction expression. Since we calculate the average mass-densities ($\rho_W = \frac{M_W}{V}$ and $\rho_B = \frac{M_B}{V}$) in the same region, the volume in Eqs. 4.1 and 4.2 cancels out giving the desired mass fraction. Hence, the solubility of water-in-butanol is given by

$$S_{WB} = \left(\frac{\rho_W}{\rho_W + \rho_B} \right) \times 100\% \dots\dots\dots 4.1,$$

and similarly the solubility of butanol-in-water can be determined through

$$S_{BW} = \left(\frac{\rho_B}{\rho_W + \rho_B} \right) \times 100\% \dots\dots\dots 4.2.$$

At room temperature, our calculations yield the values 17.2 % for the solubility of water-in-butanol and 11.4 % for the butanol-in-water. These findings are in excellent approximation with the reported values in the literature [69] and are sufficient to have proper simulations of our system and its nanodroplets structures, at least qualitatively.

3.4 MD OF WATER-BUTANOL NANODROPLETS

The spherical nanodroplets were also studied at different configuration where we observed the structures by tuning the butanol concentration at the same temperature of DFT study, T= 250K. The spherical nanodroplets were initiated and packed using Packmol package. We used a fixed number of 1000 molecules of water throughout our simulation for the spherical configurations. The canonical molecular dynamics simulation was applied for a very long time of 100ns to ensure full equilibration. The cross interactions between the atoms were also guided by the model parameters appropriately chosen in order to match the literature solubility values.

The simulation was first executed for 200 Butanol molecules at 250K temperature. The butanol concentration was then gradually increased to study the effects on the resulting structures. Confirming DFT results, our investigations revealed a Core-Shell structure for 200 Butanol molecules as presented in Fig. 11. The core-shell structure is formed such that the water molecules converge at the center surrounded by the butanol molecules.

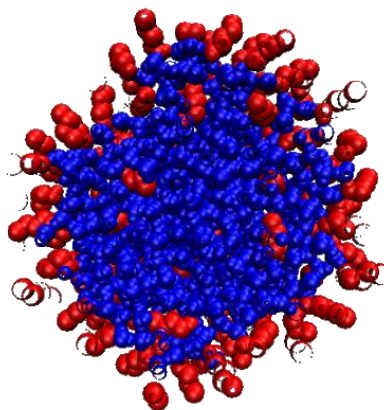


Fig. 11: Snapshot of the Core-shell Structure of the spherical nanodroplets for 200 Butanol and 100 Water molecules at $T=250\text{K}$

However, for 1000 Butanol molecules at 250K, we observed an entirely different structure, where the two components of the mixture completely separate from each other with the water molecules shrinking at one end and the butanol molecules converging to the other end and sparingly covering the water molecules as presented in Fig. 12. This structure can be called Phase separated Russian Doll-Shell (RDS) structure where the lens-on-sphere structure is coated by a thin layer of butanol.

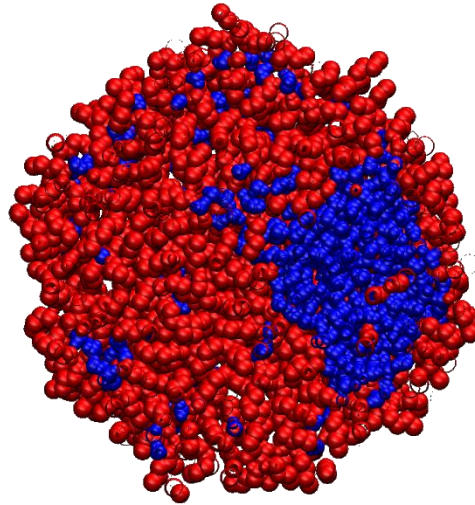


Fig. 12: Snapshot of the Phase-separation Structure of the spherical nanodroplets for 1000 Butanol and 1000 Water molecules at $T=250\text{K}$.

Figures 13a and 13b represent the map of the average local number density [$n \text{ (m}^{-3}\text{)}$] of water and butanol, respectively, around a symmetry axis that passes through the center of water-rich and butanol-rich phases in the RDS structure. Our average is carried over the time period 80-100ns.

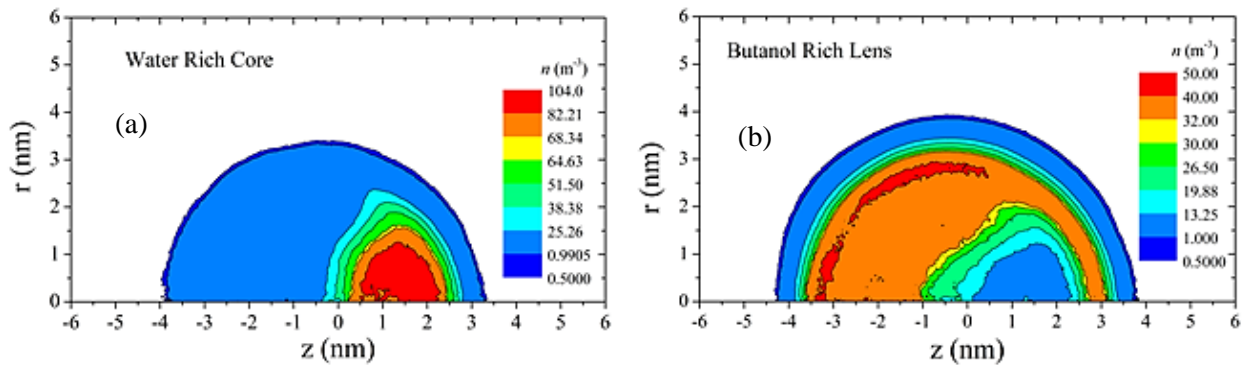


Fig. 13: Number density map around a symmetry axis connecting the center of water-rich phase and the butanol-rich phase. (a) Shows a water-rich core with diameter approximately equals 2.5 nm. (b) Shows butanol-rich lens confines the water core. The thin layer of butanol that coats the lens-on-sphere structure is partially seen in our simulation as a red strip in the butanol-rich lens.

In addition, we continued to increase the butanol concentration until we found that the two components of the mixture have thoroughly mixed with each other. For example, WM structure is vividly recognized for 3000 molecules of butanol and 1000 molecules of water at $T=250\text{K}$. The snapshot of the resulting mixture is shown in Fig. 14.

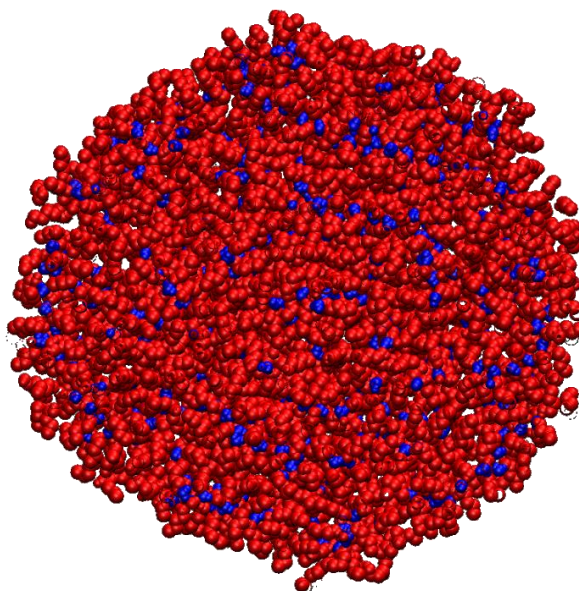


Fig. 14: Snapshot of the Well-Mixed Structure of the spherical nanodroplet for 3000 Butanol and 1000 water molecules at $T=250\text{K}$.

To study the stability of RDS structure under temperature variation, we increased the temperature for fixed butanol and water concentrations (1000 Butanol and 1000 Water molecules) and studied the nanostructure of our droplets. We found that this concentration varies gradually from the RDS region to the WM region in the phase diagram ending up with the WM nanodroplet structure as shown in Fig. 15. However, by lowering the temperature less than 250K , we expect the RDS structure becomes more pronounced as the water-rich core expands by absorbing more water molecules from the butanol-rich lens and the butanol-rich lens becomes more butanol-richer. Eventually, it is worthily to extremely decrease the temperature until the

water and butanol become completely immiscible and thereafter we can figure out whether the system pertains its RDS structure or will convert to another structure such as RD structure.

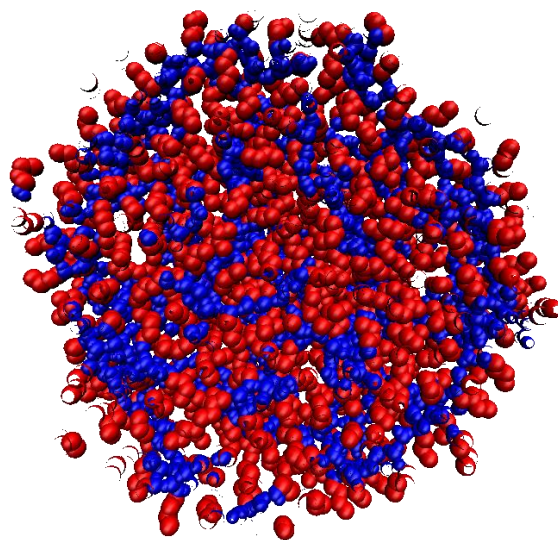


Fig. 15: Snapshot of the Well-Mixed Structure of the spherical nanodroplets for 1000 Butanol and 1000 water molecules at $T=295K$

CHAPTER FOUR

CONCLUSION AND RECOMMENDATIONS

4.1 CONCLUSIONS

We carried several canonical molecular dynamics simulations on water/butanol binary nanodroplets and proposed a model that mimics the properties of the real mixture based on experimental findings. The water-butanol mutual solubilities were computed at room temperature. Moreover, the surface tension and liquid density of the pure TraPPE butanol was computed for various temperatures in order to confirm its properties and existence.

Furthermore, we packed the nanodroplets in form of spheres centered in a larger square box and applied the canonical molecular dynamics simulation by tuning the concentration of the butanol. We observed a core-shell (CS) structure for 200 molecules of butanol and 1000 molecules of water at a temperature of 250K. We also observed a Phase-separation RDS structure for 1000 molecules of butanol and 1000 molecules of water at 250K. However, the phase separation structure converted to WM structure by increasing the temperature indicating that the solubility increased and the concentration conditions afterwards belongs to the WM region instead of the RDS region in the phase diagram. Moreover, at 250K, increasing the butanol number to 3000 molecules at constant water concentration also created a well-mixed structure.

Our results agree with the DFT study of water-alcohol nanodroplets at low butanol concentrations (CS structure) and high butanol concentrations (WM structure). However, it does not confirm the double-saddle regions in the free energy surface for moderate butanol concentrations (bi-structural region by DFT shows CS alongside WM structures) but actually it

shows a new structure combining both the CS and WM in one structure. This RDS structure suggests a wide single-saddle point region in the free energy surface where we expect the work of formation of our RDS nanodroplets to be lowest.

We could attribute this discrepancy between our MD and their DFT results to the mean-field approximation of using Yukawa potential with the classical DFT and spherical symmetry. The researchers of reference [4] started their computations from CS region and they tuned the parameter towards the bi-structural region where they keep finding the CS structure all the way cross the region. Similarly, when they moved from the WM structure toward the bi-structural region, they only saw WM structure in the bi-structural region.

Vividly, their bi-structural region is actually our RDS structure region and the binary water-butanol nanodroplets can have three different structures instead of two. For more explanations, they saw two different structures in the bi-structural region because of the mean-field limitations of their classical DFT due to using spherical coordinates with Yukawa potential. Thus, DFT can only see the density profiles between the center of the RDS water-rich core and the vapor phase toward the +Z-axis in figure 13a and WM density profiles between the center of RDS butanol-rich lens and the vapor phase toward the -Z-axis in figure 13b.

4.2 RECOMMENDATIONS

- 1) This thesis work was conducted for water/butanol mixture. Therefore, there is need to apply such simulations to the mixtures of other organic solvents and water in order to explore their various properties.

- 2) For the current work, the van der Waal parameters for water are well documented in the literature. However, the parameters for butanol need some further investigations for lower temperature.
- 3) The water/butanol mixture needs to be studied deeply at extremely high and low temperatures in order to explore some possible structures and their thermodynamic behavior at such extremities.
- 4) More study need to be performed to find wither our RDS structure is a critical nuclei or not. This is important because only those structures that reach the critical size are significant to the nucleation process.

REFERENCES

- [1] I. L. Carpenter and W. J. Hehre, "A molecular dynamics study of the hexane/water interface," *J. Phys. Chem.*, vol. 94, no. 2, pp. 531–536, Jan. 1990.
- [2] M. Meyer, M. Mareschal, and M. Hayoun, "Computer modeling of a liquid–liquid interface," *J. Chem. Phys.*, vol. 89, no. 2, p. 1067, 1988.
- [3] B. E. Wyslouzil, G. Wilemski, R. Strey, C. H. Heath, and U. Dierregswiler, "Experimental evidence for internal structure in aqueous–organic nanodroplets," *Phys. Chem. Chem. Phys.*, vol. 8, no. 1, pp. 54–57, 2006.
- [4] J.-S. Li and G. Wilemski, "A structural phase diagram for model aqueous organic nanodroplets," *Phys. Chem. Chem. Phys.*, vol. 8, no. 11, pp. 1266–70, Mar. 2006.
- [5] G. Wilemski, "Homogeneous Binary Nucleation Theory and the Structure of Binary Nanodroplets," *Nucleation Atmos. Aerosols*, no. August, pp. 267–277, 2007.
- [6] M. M. Malyshkina, "The Structure of Gasdynamic Flow in a Supersonic Separator of Natural Gas," vol. 46, no. 1, pp. 69–76, 2008.
- [7] A. Karimi and M. A. Abdi, "Selective dehydration of high-pressure natural gas using supersonic nozzles," *Chem. Eng. Process. Process Intensif.*, vol. 48, no. 1, pp. 560–568, Jan. 2009.
- [8] P. Peeters, G. Pieterse, J. Hrubý, and M. E. H. van Dongen, "Multi-component droplet growth. I. Experiments with supersaturated n-nonane vapor and water vapor in methane," *Phys. Fluids*, vol. 16, no. 7, p. 2567, Jun. 2004.
- [9] P. Peeters, G. Pieterse, and M. E. H. van Dongen, "Multi-component droplet growth. II. A theoretical model," *Phys. Fluids*, vol. 16, no. 7, p. 2575, Jun. 2004.
- [10] F. Hrahsheh and G. Wilemski, "Fluctuating structure of aqueous organic nanodroplets," in *NUCLEATION AND ATMOSPHERIC AEROSOLS: 19th International Conference*, 2013, vol. 1527, no. 1, pp. 63–66.
- [11] D. V. Spracklen, K. S. Carslaw, M. Kulmala, V.-M. Kerminen, G. W. Mann, and S.-L. Sihto, "The contribution of boundary layer nucleation events to total particle concentrations on regional and global scales," *Atmos. Chem. Phys.*, vol. 6, no. 12, pp. 5631–5648, 2006.
- [12] C. D. O'Dowd and T. Hoffmann, "Coastal New Particle Formation: A Review of the Current State-Of-The-Art," *Environ. Chem.*, vol. 2, no. 4, p. 245, 2005.
- [13] M. J. Dunn, J.-L. Jiménez, D. Baumgardner, T. Castro, P. H. McMurry, and J. N. Smith, "Measurements of Mexico City nanoparticle size distributions: Observations of new particle formation and growth," *Geophys. Res. Lett.*, vol. 31, no. 10, p. n/a–n/a, May 2004.
- [14] R. J. Charlson, J. H. Seinfeld, A. Nenes, M. Kulmala, A. Laaksonen, and M. C. Facchini, "Reshaping the Theory of Cloud Formation," *Science (80-.)*, vol. 292, no. 5524, 2001.
- [15] S. E. Schwartz, "BNL-75155-2005-BC AEROSOL, CLOUDS, AND CLIMATE

- CHANGE,” pp. 323–338, 2004.
- [16] G. B. Ellison, A. F. Tuck, and V. Vaida, “Atmospheric processing of organic aerosols,” *J. Geophys. Res. Atmos.*, vol. 104, no. D9, pp. 11633–11641, May 1999.
- [17] H. Tervahattu, J. Juhanaja, V. Vaida, A. F. Tuck, J. V. Niemi, K. Kupiainen, M. Kulmala, and H. Vehkamäki, “Fatty acids on continental sulfate aerosol particles,” *J. Geophys. Res. Atmos.*, vol. 110, no. D6, p. n/a–n/a, Mar. 2005.
- [18] G. Wilemski, B. E. Wyslouzil, R. Strey, C. H. Heath, and U. Dierregswailer, “Experimental Evidence for Internal Structure in Aqueous -- Organic Nanodroplets,” *Am. Phys. Soc. APS March Meet. March 13-17, 2006, Abstr. #R11.008*, 2006.
- [19] Y. Qiu and V. Molinero, “Morphology of Liquid–Liquid Phase Separated Aerosols,” *J. Am. Chem. Soc.*, vol. 137, no. 33, pp. 10642–10651, Aug. 2015.
- [20] D. E. Sullivan, “Interfacial density profiles of a binary van der Waals fluid,” *J. Chem. Phys.*, vol. 77, no. 5, p. 2632, 1982.
- [21] X. C. Zeng and D. W. Oxtoby, “Binary homogeneous nucleation theory for the gas–liquid transition: A nonclassical approach,” *J. Chem. Phys.*, vol. 95, no. 8, p. 5940, 1991.
- [22] V. Talanquer and D. W. Oxtoby, “Critical clusters in binary mixtures: A density functional approach,” *J. Chem. Phys.*, vol. 104, no. 5, p. 1993, 1996.
- [23] R. M. C. and T. Pakula*, “Behavior of Evaporating Droplets at Nonsoluble and Soluble Surfaces: Modeling with Molecular Resolution,” 2005.
- [24] A. Obeidat, F. Hrahsheh, and G. Wilemski, “Scattering Form Factors for Russian Doll Aerosol Droplet Models,” *J. Phys. Chem. B*, vol. 119, no. 29, pp. 9304–9311, Jul. 2015.
- [25] J. L. Schmitt, J. Whitten, G. W. Adams, and R. A. Zalabsky, “Binary nucleation of ethanol and water,” *J. Chem. Phys.*, vol. 92, no. 6, p. 3693, 1990.
- [26] R. Strey, Y. Viisanen, and P. E. Wagner, “Measurement of the molecular content of binary nuclei. III. Use of the nucleation rate surfaces for the water-n-alcohol series,” *J. Chem. Phys.*, vol. 103, no. 10, p. 4333, 1995.
- [27] T. Rodemann and F. Peters, “Experimental investigation of binary nucleation rates of water–n-propanol and water–n-butanol vapors by means of a pex-tube,” *J. Chem. Phys.*, vol. 105, no. 12, p. 5168, 1996.
- [28] B. E. Wyslouzil, C. H. Heath, J. L. Cheung, and G. Wilemski, “Binary condensation in a supersonic nozzle,” *J. Chem. Phys.*, vol. 113, no. 17, p. 7317, 2000.
- [29] G. Wilemski, “Revised classical binary nucleation theory for aqueous alcohol and acetone vapors,” *J. Phys. Chem.*, vol. 91, no. 10, pp. 2492–2498, May 1987.
- [30] R. C. Brown, R. C. Miake-Lye, M. R. Anderson, C. E. Kolb, and T. J. Resch, “Aerosol dynamics in near-field aircraft plumes,” *J. Geophys. Res. Atmos.*, vol. 101, no. D17, pp. 22939–22953, Oct. 1996.
- [31] C. Flageollet-Daniel, J. P. Garnier, and P. Mirabel, “Microscopic surface tension and

- binary nucleation,” *J. Chem. Phys.*, vol. 78, no. 5, p. 2600, 1983.
- [32] A. Laaksonen and M. Kulmala, “An explicit cluster model for binary nuclei in water–alcohol systems,” *J. Chem. Phys.*, vol. 95, no. 9, p. 6745, 1991.
- [33] A. Laaksonen, “Nucleation of binary water–n-alcohol vapors,” *J. Chem. Phys.*, vol. 97, no. 3, p. 1983, 1992.
- [34] A. S. Clarke, R. Kapral, and G. N. Patey, “Structure of two-component clusters,” *J. Chem. Phys.*, vol. 101, no. 3, p. 2432, 1994.
- [35] M. T. and M. L. Klein*, “Molecular Dynamics Study of Two-Component Systems: The Shape and Surface Structure of Water/Ethanol Droplets,” 1997.
- [36] *,† Bin Chen, ‡ and J. Ilja Siepmann, and M. L. Klein†, “Simulating the Nucleation of Water/Ethanol and Water/n-Nonane Mixtures: Mutual Enhancement and Two-Pathway Mechanism,” 2003.
- [37] M. E. M. and B. Chen*, “Unravelling the Peculiar Nucleation Mechanisms for Non-Ideal Binary Mixtures with Atomistic Simulations†,” 2005.
- [38] M. J. Osborne and D. J. Lacks, “Surface segregation in liquid mixtures with strong interspecies attraction,” *Phys. Rev. E*, vol. 70, no. 1, p. 010501, Jul. 2004.
- [39] A. K. Ray, M. Chalam, and L. K. Peters, “Homogeneous nucleation of binary vapors partially miscible in liquid state,” *J. Chem. Phys.*, vol. 85, no. 4, p. 2161, 1986.
- [40] P. R. ten Wolde and D. Frenkel, “Numerical study of gas–liquid nucleation in partially miscible binary mixtures,” *J. Chem. Phys.*, vol. 109, no. 22, p. 9919, 1998.
- [41] I. Napari and A. Laaksonen, “Gas–liquid nucleation in partially miscible systems: Free-energy surfaces and structures of nuclei from density functional calculations,” *J. Chem. Phys.*, vol. 111, no. 12, p. 5485, 1999.
- [42] I. Napari, A. Laaksonen, and R. Strey, “Density-functional studies of amphiphilic binary mixtures. I. Phase behavior,” *J. Chem. Phys.*, vol. 113, no. 10, p. 4476, 2000.
- [43] V. Talanquer and D. W. Oxtoby, “Nucleation in the presence of an amphiphile: A density functional approach,” *J. Chem. Phys.*, vol. 106, no. 9, p. 3673, 1997.
- [44] Y. Viisanen, P. E. Wagner, and R. Strey, “Measurement of the molecular content of binary nuclei. IV. Use of the nucleation rate surfaces for the n-nonane-n-alcohol series,” *J. Chem. Phys.*, vol. 108, no. 10, p. 4257, 1998.
- [45] N. Processing, “The Crucial Link Between Natural Gas Production and Its Transportation to Market,” *Energy Inf. Adm. Off. Oil ...*, 2006.
- [46] E. Fermi, J. Pasta, and S. Ulam, “Studies of nonlinear problems,” *Los Alamos Rep. LA-1940*, 1955.
- [47] B. J. Alder and T. E. Wainwright, “Studies in Molecular Dynamics. I. General Method,” *J. Chem. Phys.*, vol. 31, no. 2, p. 459, 1959.
- [48] J. B. Gibson, A. N. Goland, M. Milgram, and G. H. Vineyard, “Dynamics of Radiation

- Damage,” *Phys. Rev.*, vol. 120, no. 4, pp. 1229–1253, Nov. 1960.
- [49] A. Rahman, “Correlations in the Motion of Atoms in Liquid Argon,” *Phys. Rev.*, vol. 136, no. 2A, pp. A405–A411, Oct. 1964.
- [50] T. Schlick, “Pursuing Laplace’s Vision on Modern Computers,” Springer New York, 1996, pp. 219–247.
- [51] M. Levitt and A. Warshel, “Computer simulation of protein folding,” *Nature*, 1975.
- [52] S. Piana, J. L. Klepeis, and D. E. Shaw, “Assessing the accuracy of physical models used in protein-folding simulations: quantitative evidence from long molecular dynamics simulations,” *Curr. Opin. Struct. Biol.*, vol. 24, pp. 98–105, 2014.
- [53] K. A. Beauchamp, Y.-S. Lin, R. Das, and V. S. Pande, “Are Protein Force Fields Getting Better? A Systematic Benchmark on 524 Diverse NMR Measurements,” *J. Chem. Theory Comput.*, vol. 8, no. 4, pp. 1409–1414, Apr. 2012.
- [54] A. Raval, S. Piana, M. P. Eastwood, R. O. Dror, and D. E. Shaw, “Refinement of protein structure homology models via long, all-atom molecular dynamics simulations,” *Proteins Struct. Funct. Bioinforma.*, vol. 80, no. 8, p. n/a–n/a, 2012.
- [55] B. J. Alder and T. E. Wainwright, “Studies in Molecular Dynamics. II. Behavior of a Small Number of Elastic Spheres,” *J. Chem. Phys.*, vol. 33, no. 5, p. 1439, 1960.
- [56] L. Verlet, “Computer "Experiments" on Classical Fluids. I. Thermodynamical Properties of Lennard-Jones Molecules,” *Phys. Rev.*, vol. 159, no. 1, pp. 98–103, Jul. 1967.
- [57] J. L. Lebowitz and J. K. Percus, “Thermodynamic Properties of Small Systems,” *Phys. Rev.*, vol. 124, no. 6, pp. 1673–1681, Dec. 1961.
- [58] B. J. F.-P. and J. C. Hemminger†, “Physical Chemistry of Airborne Sea Salt Particles and Their Components,” 2000.
- [59] E. M. Knipping, M. J. Lakin, K. L. Foster, P. Jungwirth, D. J. Tobias, R. B. Gerber, D. Dabdub, and B. J. Finlayson-Pitts, “Experiments and Simulations of Ion-Enhanced Interfacial Chemistry on Aqueous NaCl Aerosols,” *Science (80-.)*, vol. 288, no. 5464, 2000.
- [60] H. El Bardouni, M. Mareschal, R. Lovett, and M. Baus, “Computer simulation study of the local pressure in a spherical liquid–vapor interface,” *J. Chem. Phys.*, vol. 113, no. 21, p. 9804, 2000.
- [61] P. Schofield, “The statistical theory of surface tension,” *Chem. Phys. Lett.*, vol. 62, no. 3, pp. 413–415, 1979.
- [62] L. Martínez, R. Andrade, E. G. Birgin, and J. M. Martínez, “PACKMOL: a package for building initial configurations for molecular dynamics simulations,” *J. Comput. Chem.*, vol. 30, no. 13, pp. 2157–64, Oct. 2009.
- [63] H. J. C. Berendsen, D. van der Spoel, and R. van Drunen, “GROMACS: A message-passing parallel molecular dynamics implementation,” *Comput. Phys. Commun.*, vol. 91,

- no. 1–3, pp. 43–56, Sep. 1995.
- [64] S. Nosé, “A unified formulation of the constant temperature molecular dynamics methods,” *J. Chem. Phys.*, vol. 81, no. 1, p. 511, 1984.
- [65] M. Gharibeh, Y. Kim, U. Dierregsweiler, B. E. Wyslouzil, D. Ghosh, and R. Strey, “Homogeneous nucleation of n-propanol, n-butanol, and n-pentanol in a supersonic nozzle,” *J. Chem. Phys.*, vol. 122, no. 9, p. 094512, 2005.
- [66] A. Hemmen and J. Gross, “Transferable Anisotropic United-Atom Force Field Based on the Mie Potential for Phase Equilibrium Calculations: n-Alkanes and n-Olefins,” *J. Phys. Chem. B*, vol. 119, no. 35, pp. 11695–11707, Sep. 2015.
- [67] W. L. Jorgensen, D. S. Maxwell, and J. Tirado-Rives, “Development and Testing of the OPLS All-Atom Force Field on Conformational Energetics and Properties of Organic Liquids,” *J. Am. Chem. Soc.*, vol. 118, no. 45, pp. 11225–11236, Jan. 1996.
- [68] † Bin Chen, ‡ and Jeffrey J. Potoff, and J. I. Siepmann*, “Monte Carlo Calculations for Alcohols and Their Mixtures with Alkanes. Transferable Potentials for Phase Equilibria. 5. United-Atom Description of Primary, Secondary, and Tertiary Alcohols,” 2001.
- [69] R. Stephenson and J. Stuart, “Mutual binary solubilities: water-alcohols and water-esters,” *J. Chem. Eng. Data*, vol. 31, no. 1, pp. 56–70, Jan. 1986.

Vitae

A. PERSONAL DATA

NAME : Yakubu Sani Wudil.
NATIONALITY : Nigerian.
PLACE OF BIRTH : Zango Wudil, Wudil L. G. A., Kano State.
DATE OF BIRTH : 21st January, 1991.
MARRITAL STATUS : Single.
RELIGION : Islam
TRIBE : Hausa
Email : yswudil@yahoo.com
MOBILE PHONE : +966532449461, +2347034373844

B. SCHOOLS ATTENDED WITH DATES

2014-2016 : King Fahd university of Petroleum and Minerals, Dhahran, Saudi Arabia
2008-2012 : Bayero University, Kano.
2008 : Martaba School of Information Technology, Kano
2005 –2008 : Dawakin Kudu Science College, Kano
2002 –2005 : Government Secondary School Kwankwaso.
1996-2002 : Wudil Model primary school.

C. ACADEMIC AND PROFFESIONAL QUALIFICATIONS WITH DATES.

2016 : Master's degree in Physics
2012 : Bachelor Degree in physics (B.Sc Physics), **First Class**
2008 : Certificate in Information Technology (C.I.T), Upper Credit

- 2008 : Senior Secondary School leaving certificate (S.S.C.E)
- 2005 : Junior Secondary School Leaving Certificate (J.S.C.E)
- 2002 : Primary School Leaving Certificate.

D. DISTINCTIONS AND AWARDS.

- 2014 : K.F.U.P.M. Master's Scholarship for exceptional students
- 2013 : Best Graduating Student in the University at the 30th convocation ceremony of Bayero University, Kano.
- 2013 : Best Graduating Student in physics Department, **(First Class)**
- 2013 : Best Graduating Student in the Faculty of Sciences
- 2010 – 2012 : Federal Government Merit (Scholarship) Award in Physics.
- 2009 : Bayero University, Kano Merit scholarship for the Best student (level I) in the 2008/2009 examination in physics.
- 2010 : Bayero University, Kano Merit scholarship for the Best student (level II) in the 2009/2010 examination in physics
- 2011 : Bayero University, Kano Merit scholarship for the Best student (level III) in the 2010/2011 examination in physics
- 2012 : Award of excellence as the Best Student (level IV) in the Faculty of Science by the National association of Science Students, B.U.K chapter
- 2012 : Award of excellence as the Best Student of physics department by the National Association of Physics Students, B.U.K chapter